An All-Purpose Full-Vectorial Finite Element Model for Arbitrarily Shaped Crossed-Gratings

Guillaume Demésy*,[1], Frédéric Zolla[1], André Nicolet[1], and Mireille Commandré[1]
[1] Institut Fresnel, Université Aix-Marseille III, École Centrale de Marseille, France
*Corresponding author: guillaume.demesy@fresnel.fr

Abstract: We demonstrate the accuracy of the Finite Element Method (FEM) to characterize an arbitrarily shaped crossed-grating in a multilayered stack illuminated by an arbitrarily polarized plane wave under oblique incidence. To our knowledge, this is the first time that 3D diffraction efficiencies are calculated using the FEM. The method has been validated using classical cases found in the literature. Finally, to illustrate the independence of our method towards the shape of the diffractive object, we present the global energy balance resulting of the diffraction of a plane wave by a lossy thin torus crossed-grating.

Keywords: Electromagnetism, Diffraction, Crossed grating, Arbitrary Geometry

1 Introduction

To date, numerical methods are devoted to the calculation of the repartition of the energy resulting from the diffraction of a plane wave by a crossed-grating : the Rigorous Coupled-Wave Method (RCWA [1]), also known as the Fourier Modal Method (FMM [2]) , the differential method [3], the Chandezon (C) method [4], the Rayleigh method [5] and the method of variation of boundaries [6]. Some of them appear to require some memory and time consuming adjustments depending on whether the grating presents, for instance, abrupt sections or a strong index modulation. The present paper is aimed at introducing the resolution of this diffraction vectorial problem through a formulation fully based on the FEM with 2^{nd} edge elements and relying on the the same principles developed in [7]. By presenting a global energy balance in the case of a lossy torus–shaped diffractive object, we finally emphasize the independence of our method towards the geometry.

We denote by $\mathbf{x}$, $\mathbf{y}$ and $\mathbf{z}$, the unit vectors of the axes of an orthogonal coordinate system $Oxyz$. We only deal with time-harmonic fields; consequently, the electric and magnetic fields are represented by the complex vector fields $\mathbf{E}$ and $\mathbf{H}$, with a time dependance in $\exp(-i\,\omega\,t)$. Besides, in this paper, for the sake of simplicity, the materials are assumed to be isotropic and therefore are optically characterized by there relative permittivity ε_r and relative permeability μ_r. It is of importance to note that lossy materials can be studied (the permittivity and permeability are represented by possibly complex valued functions). Moreover the method used in this paper does work irrespective of whether the materials are homogeneous: the permittivity (resp. permeability) can vary continuously (gradient index gratings) or discontinuously (step index gratings). The bigratings that we are dealing with are made of three distinct regions as suggested in Fig. 1:

- *The superstrate (above the translucent white plane in Fig. 1)* ($z > h$) which is supposed to be homogeneous, isotropic and lossless and characterized solely by its relative permittivity ε^+ and its relative permeability μ^+ and we denote $k^+ := k_0\sqrt{\varepsilon^+\mu^+}$, where $k_0 := \frac{\omega}{c}$,

- *The substrate (bottom region in Fig. 1)* ($z < 0$) which is supposed to be homogeneous and isotropic and therefore characterized by its relative permittivity ε^- and its relative permeability μ^- and we denote $k^- := k_0\sqrt{\varepsilon^-\mu^-}$,

- *The groove region* ($0 < z < h$) which can be heterogeneous and thus characterized by the scalar fields $\varepsilon^g(x,y,z)$ and $\mu^g(x,y,z)$. The groove periodicity along the x–axis is supposed to be equal to the periodicity along the y–axis and will be denoted d in the sequel.

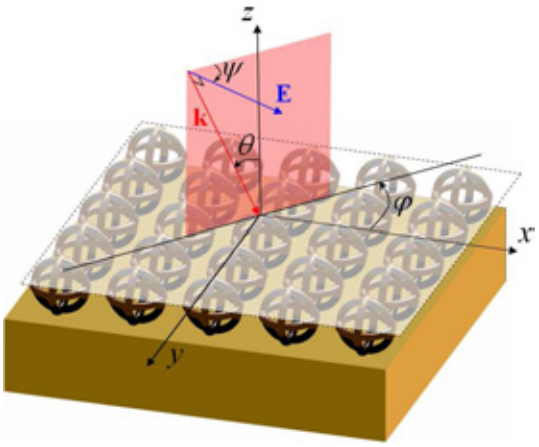

Figure 1: Set up of the problem and notations.

This bigrating is illuminated by an incident plane wave of wave vector $\mathbf{k}^+$ defined by the angles θ and φ ($\mathbf{k}^+ = k^+ (\sin\theta\,\cos\varphi\,\mathbf{x} + \sin\theta\,\sin\varphi\,\mathbf{y} + \cos\theta\,\mathbf{z})$) and whose the electric field $\mathbf{E}^0$ is linearly polarized along the direction defined by the unit vector $\mathbf{A}^0$ ($\mathbf{E}^0 = \mathbf{A}^0 \exp(i\mathbf{k}^+ \cdot \boldsymbol{r})$, with $\mathbf{A}^0 = (\cos\Psi\,\cos\theta\,\cos\varphi - \sin\Psi\,\sin\varphi)\,\mathbf{x} + (\cos\Psi\,\cos\theta\,\sin\varphi + \sin\Psi\,\cos\varphi)\,\mathbf{y} - (\cos\Psi\,\sin\theta)\,\mathbf{z}$), where Ψ is the polarization angle. The problem of diffraction that we address in this paper is therefore to find Maxwell equation solutions in harmonic regime *i.e.* the unique solution $\mathbf{E}$ of:

$$\mathscr{M}_{\varepsilon_r,\mu_r}(\mathbf{E}) := -\,\mathbf{curl}\left(\mu_r^{-1}\,\mathbf{curl}\,\mathbf{E}\right) + k_0^2\,\varepsilon_r\,\mathbf{E} = 0\ , \tag{1}$$

such that the diffracted field satisfies an *Outgoing Waves Condition* (OWC [8]) and where $\mathbf{E}$ is a quasi-periodic functions with respect to x and y co-ordinates.

In what follows, one summarizes and generalizes the method developed in [7] for the two-dimensional case. In its initial form, the problem of diffraction summed up by Eq.(1) is not well suited to the Finite Element Method. In order to overcome this difficulty, we propose to split the unknown function $\mathbf{E}$ into a sum of two functions $\mathbf{E}_1$ and $\mathbf{E}_2^d$, the first term being known as a closed form and the latter being a solution of a problem of radiation whose sources are localized within the obstacles.

We have assumed that outside the groove region (cf. Fig. 1), the scalar field ε_r and μ_r are constant and equal respectively to ε^- and μ^- in the substrate ($z < 0$) and equal respectively to ε^+ and μ^+ in the superstrate ($z > h$). With such notations, ε_r and μ_r are therefore defined as follows:

$$\xi_r(x,y,z) := \begin{cases} \xi^+ & \text{for} \quad z > h \\ \xi^g(x,y,z) & \text{for} \quad h > z > 0 \\ \xi^- & \text{for} \quad z < 0 \end{cases} \tag{2}$$

where $\xi = \{\varepsilon, \mu\}$. It is now appropriate to introduce two auxiliary scalar fields, namely ε_1 and μ_1 :

$$\xi_1(x,y,z) := \begin{cases} \xi^+ & \text{for} \quad z > 0 \\ \xi^- & \text{for} \quad z < 0 \end{cases}\ , \tag{3}$$

where $\xi = \{\varepsilon, \mu\}$, these quantities corresponding, of course, to a simple plane interface. Finally, we denote $\mathbf{E}_0^0$ the vector field which is equal to the incident field $\mathbf{E}^0$ in the superstrate and vanishes elsewhere

$$\mathbf{E}_0^0(x,y,z) := \begin{cases} \mathbf{E}_0 & \text{for} \quad z > h \\ 0 & \text{for} \quad z < h \end{cases}\ . \tag{4}$$

We are now in a position to define more precisely the problem of diffraction that we are dealing with. The function $\mathbf{E}$ is the unique solution of Eq. (1) such that $\mathbf{E}^d := \mathbf{E} - \mathbf{E}_0^0$ satisfies an OWC. In order to reduce this problem of diffraction to a radiation problem, an intermediate vector field is necessary. This vector field, called $\mathbf{E}_1$, is defined as the unique solution of the equation:

$$\mathscr{M}_{\varepsilon_1,\mu_1}(\mathbf{E}_1) = 0 \tag{5}$$

such that $\mathbf{E}_1^d := \mathbf{E}_1 - \mathbf{E}_0^0$ satisfies an OWC. The vector field $\mathbf{E}_1$ corresponds thus to *an annex problem* associated to a simple interface and can be solved in closed form and *from now on is considered as a known vector field.* A third and last field denoted $\mathbf{E}_2^d$ has to be introduced as mentioned above; this field is simply defined as the difference between $\mathbf{E}$ and $\mathbf{E}_1$: $\mathbf{E}_2^d := \mathbf{E} - \mathbf{E}_1 = \mathbf{E}^d - \mathbf{E}_1^d$. It then appears that this latest field satisfies an OWC, which is of prime importance to use Perfectly Matched Layers (PML [9]). As a result, by making use of Eq. (5), the Eq. (1) becomes:

$$\mathscr{M}_{\varepsilon_r,\mu_r}(\mathbf{E}_2^d) = -\mathscr{M}_{\varepsilon_r,\mu_r}(\mathbf{E}_1) = -\mathscr{M}_{\varepsilon_r-\varepsilon_1,\mu_r-\mu_1}(\mathbf{E}_1)\ , \tag{6}$$

where the right hand member is a vector field which may be interpreted as a *known source term whose support is localized only within the groove region.* The problem of radiation summed up in Eq. (6) is solved by using both PML at the bottom and at the top of the meshed domain and by taking into account the quasiperiodicity conditions on lateral bounds

on the same area via Bloch conditions [10]. The cell is meshed using second order tetrahedral edge elements [11]. In the following numerical examples, the maximum element size is set to $\lambda/(8\sqrt{|\Re e(\varepsilon)|})$. The final algebraic system is solved using a direct solver (PARDISO).

2 Energetic considerations

2.1 Diffraction efficiencies

The FEM allows to obtain directly the complex components of $\mathbf{E}^d$ at each point of the computational domain.

$\mathbf{E}^d$, being defined as a difference between two quasi-periodic vector fields, is quasiperiodic with respect to x and y co-ordinates and can be expanded as a Rayleigh expansion:

$$E_x^d(x,y,z) = \sum_{(n,m)\in\mathbb{Z}^2} u_{n,m}^{d,x}(z)\, e^{-i\,(\alpha_n\, x+\beta_m\, y)} \tag{7}$$

with $\alpha_n = \alpha_0 + \frac{2\,\pi}{d_x}\, n$, $\beta_m = \beta_0 + \frac{2\,\pi}{d_y}\, m$ and

$$u_{n,m}^{d,x}(z) = \frac{1}{d_x\, d_y} \int_{-d_x/2}^{d_x/2} \int_{-d_y/2}^{d_y/2} E_x^d(x,y,z)\, e^{-i\,(\alpha_n\, x+\beta_m\, y)}\, dx\, dy \tag{8}$$

Introducing this decomposition into the Helmholtz equation scalarly verified by each component of $\mathbf{E}^d$ everywhere but in the groove region leads to the expression of the Rayleigh coefficients in the superstrate and the substrate:

$$u_{n,m}^{d,x}(z) = e_{n,m}^{x,p}\, e^{\,-i\,\gamma_{n,m}^{+}\, z} + e_{n,m}^{x,c}\, e^{\,i\,\gamma_{n,m}^{+}\, z} \tag{9}$$

with $\gamma_{n,m}^{\pm^2} = k^{\pm^2} - \alpha_n^2 - \beta_m^2$, where $\gamma_{n,m}$ (or $-i\,\gamma_{n,m}$) is defined positive. $u_{n,m}^{d,x}$ corresponds to the sum of a propagative plane wave and a couterpropagative plane wave. Consequently, the OWC impose:

$$\forall (n,m)\in\mathbb{Z}^2 \begin{cases} e_{n,m}^{x,p} = 0 \quad \text{for } z > H \\ \\ e_{n,m}^{x,c} = 0 \quad \text{for } z < 0 \end{cases} \tag{10}$$

Eq. 8 allows to determine $e_{n,m}^{x,c}$ (resp. $e_{n,m}^{x,p}$) by double numerical integration of a cutting of the field E_x^d at a fixed altitude z_c in the superstrate (resp. substrate). The components E_y^d and E_z^d can be discomposed exactly the same way, which leads to complex numerical values for $e_{n,m}^{y,\{c,p\}}$ and $e_{n,m}^{z,\{c,p\}}$.

Finally, we deduce the transmitted and reflected diffraction efficiencies defined by the following expressions, close to the one known in the scalar case[8]:

$$\begin{cases} \forall z_c > H \quad R_{n,m} = \frac{\gamma_{n,m}^{+}}{\gamma_0}\, \mathbf{e}_{n,m}^{c}(z_c) \cdot \overline{\mathbf{e}_{n,m}^{c}(z_c)} \\ \\ \forall z_c < 0 \quad T_{n,m} = \frac{\gamma_{n,m}^{-}}{\gamma_0}\, \mathbf{e}_{n,m}^{p}(z_c) \cdot \overline{\mathbf{e}_{n,m}^{p}(z_c)} \end{cases} \tag{11}$$

with $\mathbf{e}_{n,m}^{\{c,p\}} = e_{n,m}^{x,\{c,p\}}\, \mathbf{x} + e_{n,m}^{y,\{c,p\}}\, \mathbf{y} + e_{n,m}^{z,\{c,p\}}\, \mathbf{z}$.

2.2 Joule loss

Let us consider a lossy dielectric material characterized by its complex permittivity denoted $\varepsilon_r = \varepsilon' + \varepsilon''\, i$, its complex permeability $\mu_r = \mu' + \mu''\, i$ and the normal outward unit vector $\mathbf{n}$ to its surface S enclosing its volume Ω. Let us assume that there is not any magnetic dissipation for this material, which amounts to $\mu'' = 0$.

In the isotropic case, without any current, Joule losses, denoted Q, can be expressed as:

$$Q = \frac{1}{2} \int_{\Omega} \omega\, \varepsilon''\, \mathbf{E} \cdot \overline{\mathbf{E}}\, \mathrm{d}\Omega \tag{12}$$

Volumes and normal outward vectors being implicitly defined when dealing with the FEM, this quantity can be easily obtained once the vector field $\mathbf{E}$ is known at each point of the computational domain.

Finally, knowing the diffraction efficiency of each propagative order (n,m) and the losses inside each lossy material, a complete energy balance of the diffraction problem can be made:

$$\sum_{n,m} R_{n,m} + \sum_{n,m} T_{n,m} + Q = 1 \tag{13}$$

In the next section, we present three numerical illustrations, numerically validated using both values found in the bibliography and a global energy balance.

3 Numerical validation of the method

3.1 Pyramidal crossed grating

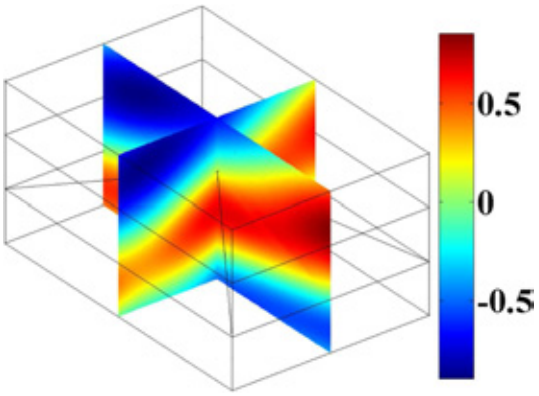

Figure 2: $\Re e\,(E_y)$ in V/m.

The numerical results obtained with the FEM applied to the pyramidal configuration (Fig. 2) show good agreement with the C method [4, 12], the Rayleigh method [5] and the RCWA [13] as shown in Table 1. Note that the diffractive pattern has oblique sides. The grating parameters are : $\varphi = \theta = 0°$ and $\psi = 45°$, $h = \lambda$ and $d_x = d_y = 5\sqrt{2}/4\,\lambda$, $\varepsilon^+ = 1$ and $\varepsilon^- = \varepsilon^g = 2.25$.

	C [4]	RM [5]	RCWA [13]	C [12]	3D FEM
$R_{-1.0}$	0.00254	0.00207	0.00246	0.00249	0.00251
$R_{0.0}$	0.01984	0.01928	0.01951	0.01963	0.01938
$T_{-1.-1}$	0.00092	0.00081	0.00086	0.00086	0.00087
$T_{0.-1}$	0.00704	0.00767	0.00679	0.00677	0.00692
$T_{-1.0}$	0.00303	0.00370	0.00294	0.00294	0.00299
$T_{0.0}$	0.96219	0.96316	0.96472	0.96448	0.96447
$T_{1.0}$	0.00299	0.00332	0.00280	0.00282	0.00290
TOTAL	0.99855	1.00001	1.00008	0.99999	1.00004

Table 1: Comparison with other methods[4, 5, 13, 12] and energy balance.

3.2 Circular apertures in a lossy layer

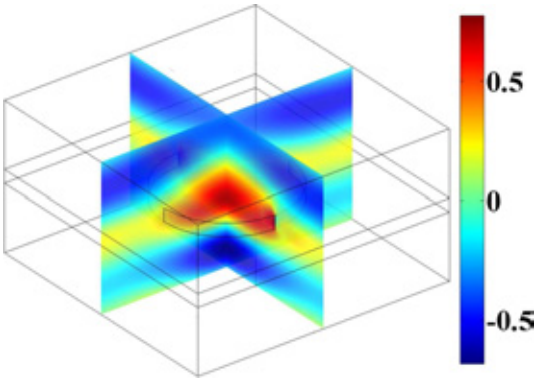

Figure 3: $\Re e\,(E_y)$ in V/m.

Compared to the results obtained with the FMM [2], the Differential Method (DM[1]) and the RCWA [14] in a lossy case (cf. Fig. 4), the FEM still gives pertinent results (with $\lambda_0 = 500$nm, $\varphi = \theta = 0°$ and $\psi = 45°$, $h = 50$nm and $d_x = d_y = 1$µm, $\varepsilon^+ = 1$, $\varepsilon^g = 0.8125 + 5.25\,i$ and $\varepsilon^- = 2.25$). Note that the geometry has vertical edges.

	RCWA [14]	FMM [2]	DM [1]	3D FEM
$R_{0.0}$	0.24657	0.24339	0.24420	0.24415
$\sum_{n=-2}^{+2}\sum_{m=-2}^{+2} T_{n,m}$	–	–	–	0.29110
$\sum_{n=-1}^{+1}\sum_{m=-1}^{+1} R_{n,m}$	–	–	–	0.26761
Q	–	–	–	0.44148
TOTAL	–	–	–	1.00019

Table 2: Comparison with other methods[14, 2, 1] and energy balance.

3.3 Bi-sinusoidal grating

In this example, the surface of the grating is given by the function f defined by :

$$f(x,y) = \frac{h}{4}\left[\cos\left(\frac{2\,\pi\,x}{d}\right) + \cos\left(\frac{2\,\pi\,y}{d}\right)\right] \tag{14}$$

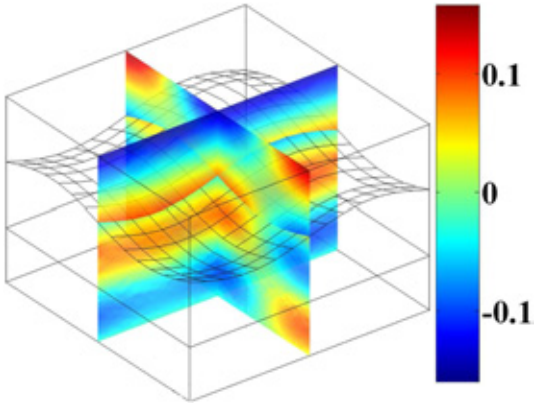

Figure 4: $\Re e\,(E_z)$ in V/m.

The grating parameters are : $\lambda_0 = 0.83$, $\varphi_0 = 0\,°$, $\theta_0 = 0\,°$, $\psi_0 = 0\,°$, $d_x = 1$, $d_y = 1$, $h = 0.2$ (cf. Eq. (14)) $\varepsilon^+ = 1$, $\varepsilon^- = 4$ and $\varepsilon^g = 4$.

	MVB[6]	FEM
$R_{-1,0}$	0.01044	0.01164
$R_{0,-1}$	0.01183	0.01165
$T_{-1,-1}$	0.06175	0.06299
$\sum_{n=-2}^{+2}\sum_{m=-2}^{+2} \Re e(R_{n,m})$	-	0.10685
$\sum_{n=-2}^{+2}\sum_{m=-2}^{+2} \Re e(T_{n,m})$	-	0.89121
TOTAL	-	0.99806

Table 3: Comparison with another method[6] and energy balance.

In order to define the geometry of this model, the bi-sinusoid has been sampled (15×15 points), converted into a standard 3D file format and merged into the other subdomains of the cell. This sampling accounts for the slight differences with the results found with the Method of Variation of Boundaries (MVB) developed by Bruno *et al.*[6] (1993). This way to define geometries thanks to standard CAD (Computer-Assisted Design) objects is very flexible.

4 Diffraction by a strongly lossy torus

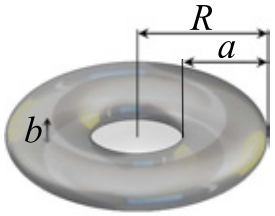

Figure 5: Lossy torus.

Finally, we consider a grating made of lossy toruses as shown Fig. 5. The implementation of this complex geometry with other numerical method is possible, but not as straightforward as with the FEM. The grating parameters are : $\varphi = \theta = \psi = 0°$, $d_x = d_y = 0.3$, $a = 0.1$, $b = 0.05$, $R = 0.15$, $\varepsilon^+ = 1$, $\varepsilon^- = 2.25$. Moreover, the difficulty of this case is increased by choosing a value of ε^g so that the skin depth $\delta \approx b$, which maximises losses. For instance, with $\varepsilon^g = -21 + 20\,i$, losses Q are of the same order of magnitude as R or T.

FEM 3D	$\theta = 0°$	$\theta = 40°$
$R_{0,0}$	0.36376	0.27331
$T_{0,0}$	0.32992	0.38191
Q	0.30639	0.34476
TOTAL	1.00007	0.99998

Table 4: Energy balance of the problem (cf. Fig. 5).

5 Conclusion

We developed a new formulation of the FEM adapted to the rigorous study of the diffraction of an arbitrarily polarized plane wave by a crossed grating. The method principle remains independent of the geometry and the number of diffractive pattern. It relies on a rigorous treatment of the plane wave sources problem through an equivalent radiation problem with localized sources. Bloch conditions and PML have been implemented in order to rigorously truncate the computational domain.

We compare the diffraction efficiencies of various crossed gratings (oblic/vertical edges and lossy/lossless constitutive materials for the diffractive pattern). To our knowledge, this is the first time that numerical values of diffraction efficiencies of crossed gratings are calculated using a formulation of the FEM entirely based on second order vectorial elements.

The main advantage of this method is its complete generality with respect to the studied geometries and the material properties. Nowadays, the efficiency of the numerical algorithms for sparse matrix algebra together with the available power of computers and the fact that the problem reduces to a basic cell with a size of a small number of wavelengths make the 3D problem very tractable as proved here.

Furthermore, this case can be easily extended to the case of a crossed grating embedded in a multilayered dielectric stack. The generalization to the case of an arbitrary anisotropic diffractive object is straightforward. Studies are in progress in these directions.

References

[1] Schuster, T., Ruoff, J., Kerwien, N., Rafler, S. and Osten, W., "Normal vector method for convergence improvement using the RCWA for crossed gratings," *J. Opt. Soc. Am. A* **24:9**, pp. 2880–2890, 2007.

[2] L. Li, "New formulation of the Fourier modal method for crossed surface-relief gratings," *J. Opt. Soc. Am. A* **14:10**, pp. 2758–2767, 1997.

[3] D. Maystre and M. Neviere, "Electromagnetic theory of crossed gratings," *J. of Optics* **9**, pp. 301–306, 1978.

[4] G. Derrick, R. McPhedran, D. Maystre, and M. Nevière, "Crossed gratings: A theory and its applications," *Appl. Phys. B* **18**(1), pp. 39–52, 1979.

[5] J. Greffet, C. Baylard, and P. Versaevel, "Diffraction of electromagnetic waves by crossed gratings: a series solution," *Opt. Lett* **17**, pp. 1740–1742, 1992.

[6] O. P. Bruno and F. Reitich, "Numerical solution of diffraction problems: a method of variation of boundaries. III. doubly periodic gratings," *J. Opt. Soc. Am. A* **10:12**, pp. 2551–2562, 1993.

[7] Demsy, G., Zolla, F.,Nicolet, A.,Commandr, M., and Fossati, C., "The finite element method as applied to the diffraction by an anisotropic grating," *Opt. Express* **15**, pp. 18089–18102, 2007.

[8] R. Petit, *Electromagnetic Theory of Gratings*, Springer Verlag, Berlin, 1980.

[9] A. N. Y. O. Agha, F. Zolla and S. Guenneau, "On the use of PML for the computation of leaky modes: an application to gradient index MOF," *COMPEL* **27**, pp. 95–109, 2008.

[10] C. G. A. Nicolet, S. Guenneau and F. Zolla, "Modeling of electromagnetic waves in periodic media with finite elements," *J. Comput. Appl. Math.* **168**(1-2), pp. 321–329, 2004.

[11] T. V. Yioultsis and T. D. Tsiboukis, "Development and implementation of second and third order vector finite elements in various 3-D electromagntic field problems," *IEEE Trans. Magnetics* **33**(2), pp. 1812–1815, 1997.

[12] G. Granet, "Reformulation of the lamellar grating problem through the concept of adaptive spatial resolution," *J. Opt. Soc. Am. A* **16**(10), pp. 2510–2516, 1999.

[13] R. Bräuer and O. Bryngdahl, "Electromagnetic diffraction analysis of two-dimensional gratings," *Opt. Communications* **100**(1-4), 1993.

[14] Moharam, M.G., Grann, E.B., Pommet, D.A. and Gaylord, T.K., "Formulation for stable and efficient implementation of the rigorous coupled-wave analysis of binary gratings," *J. Opt. Soc. Am. A* **12:5**, pp. 1068–1076, 1995.